

CSEM based Anisotropy trends in the Barents Sea.

Slim Bouchrara^{}, Lucy MacGregor, Amanda Alvarez, Michelle Ellis, Rolf Ackermann, Paola Newton, Robert Keirstead, Alburto Rusic, Yijie Zhou and Hung-Wen Tseng*

Summary

Electrical anisotropy has a strong effect on CSEM data (Ramananraona et al, 2011), and understanding this effect is key in ensuring robust survey design and well constrained data analysis (MacGregor & Tomlinson, 2014). Electrical anisotropy can also provide key information that can be used to understand regional variations in rock physics properties as well as provide possible indications to geological drivers in an area, such as uplift. To date there have been no systematic regional studies of electrical anisotropy in background geological structure. Addressing this need, by investigating electrical anisotropy variations across the Barents Sea is one of the main goals of the industry funded ERA consortium.

Bulk anisotropy values were derived from CSEM data for each of the major stratigraphic units across the Barents Sea. This was achieved by performing 1D anisotropic inversion of CSEM data acquired around well bores, and tying the horizontal resistivity to the induction log measurements from these wells. Results were then mapped and regional trends are investigated. The modelling confirms the presence of high electrical anisotropy ratios in the Barents Sea area and a correlation between anisotropy ratio and formation age: In general the older the formation, the higher the anisotropy ratio. Although resistivity varies regionally, the variation in anisotropy ratio is less pronounced.

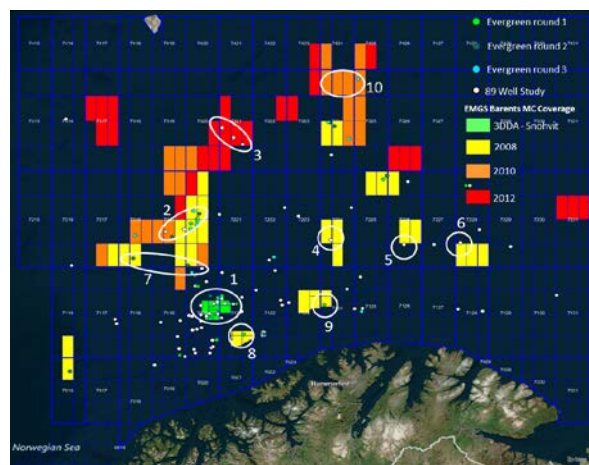


Figure 1: Map of the Barents Sea highlighting the locations of the areas covered by the anisotropy analysis (white circles).

Introduction

The anisotropy analysis covers multiple Barents Sea areas and includes 20 drilled wells. The wells included in this study have been subdivided in 10 different groups based on their geographical location (Table 1). Note that in area 10 (Hoop) no wells were available, and results are based solely on CSEM data. For each area CSEM data were inverted to determine resistivity and anisotropy values.

Area	1 (Snohvit)	2	3	4	5
Wells	7121/4-1 7120/9-1 7120/6-1 7121/4-2 7120/9-2 7120/6-2S	7220/8-1 7219/9-1 7219/8-1S 7321/9-1	7321/7-1 7321/8-1	7224/7-1	7226/11-1
Area	6	7	8	9	10 (Hoop)
Wells	7228/7-1A 7218/11-1 7220/10-1	7120/2-1 7212/9-1	7124/4-1S	PL615-1 PL615-2	

Table 1: List of wells within each ERA group.

1D Inversion of CSEM Data

The 1D modeling has been undertaken using an Occam-based 1D inversion algorithm (Constable et al, 1987). Tests using multiple inversion parameterizations and using inline-only and various inline/offline azimuthal contents of both synthetic and real survey data to determine a robust workflow were also conducted. Both CMP (common midpoint) and receiver-gather datasets were considered. All tests produced consistent models, and so the inversion work was performed using the inline only data for all receivers around the well locations, on a per-arm (either incoming or outgoing tow), per-receiver basis. The goal of the study was to determine bulk resistivity within major stratigraphic units, and therefore the inversion was stratigraphically constrained by defining one inversion cell per significant (thicker than 100 m) stratigraphic unit, using the tops at the nearest well or the seismic depth horizons. Additional constraint in the form of a regularisation break was introduced at the top of the reservoir interval for receivers near significant hydrocarbon discoveries, allowing for a sharp change in resistivity at the hydrocarbon interface.

CSEM based Anisotropy trends in the Barents Sea.

Example: Area 2

Three separate CSEM surveys were acquired in area 2 (Figure 2) between 2008 and 2010. Five wells coincide with these three surveys, of which only three have been released at the time of writing. Well 7219/8-1S is a dry well located in Bjørnøya Sør area west of the Veslemy high. Well 7219/9-1 is located in the Bjørnøya Sør area between Veslemy high and Polheim sub-platform. Three reservoir rocks (Stø, Nordmela and Tubåen) are all water-bearing with residual hydrocarbons. Finally, well 7220/8-1 (also referred to as Skrugard) targets the Skrugard fault block within the Bjørnøyna fault complex. The reservoir rocks are oil and gas-bearing and hydrocarbons were found in the Stø and Nordmela formations.

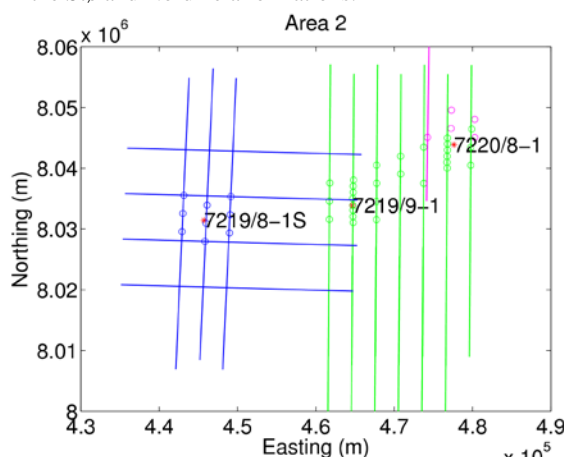


Figure 2: Map showing the CSEM acquisition surveys in Area 2. Three surveys between 2008 and 2010 were acquired (blue, green and magenta). Circles indicate receiver locations at which data were available for the study.

1D inversion analysis was carried out for all three wells using available source-receiver ranges and four frequencies chosen from those available in each survey to give optimum sub-surface sensitivity. It is important to note that since source-receiver ranges and frequencies affect the depth to which CSEM data is sensitive, comparison between the inversion results must be done with care. As a result, inverted resistivity and anisotropy are therefore best constrained in the shallower layers and uncertainty increases with depth.

There is generally a good fit of the inverted model response to the acquired CSEM data. The horizontal resistivity derived from the stratigraphically constrained 1D inversion shows very good agreement with the horizontal resistivity measured at the well locations even though no constraint was applied to the values of horizontal and vertical resistivities during the inversion process (Figure 3). This good well tie builds confidence in the inverted vertical

resistivity and the corresponding electrical anisotropy. In general, anisotropy ratios are below 5 for all the different stratigraphical units, with an average anisotropy around 2.5 for the shallow sediments (Torsk formation). The ratio increases to around 3.5 for the Kolmule interval. The Stø formation has an anisotropy ratio of 4 near well 7219/9-1 but is too deep for an accurate anisotropy measure near well 7219/8-1S.

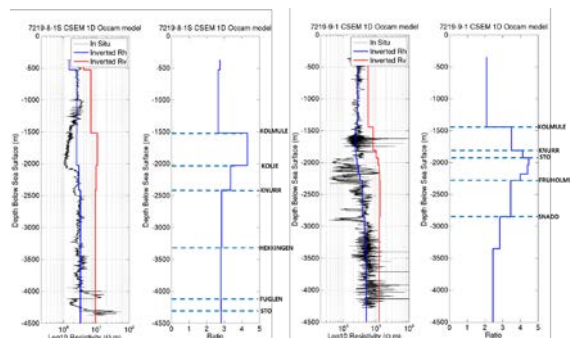


Figure 3: Comparison of the inverted horizontal and vertical resistivities from two dry wells in Area 2: well 7219/8-1S and well 7219/9-1. Left plots: the inversion models for the north arm of receiver 01Rx006a near well 7219/8-1S (the black curve is the in situ well log, the blue and red models are the inverted horizontal and vertical resistivities) and the corresponding anisotropy ratio. Right plots: the inversion models for the north arm of receiver 01Rx074a near well 7219/9-1 (with the same colour scheme as plot 1).

Figure 4 shows the models obtained from 1D anisotropic inversion of CSEM data from four different receivers located around well 7219/9-1 and so illustrates the variability in the results obtained around a single well log location. Some degree of variability between results is expected, since data from each receiver samples a different portion of a 3D earth structure, and is interpreted using a 1D approximation. Nevertheless, studies in 2D and 3D suggest that the 1D approximation is robust in this case when bulk background resistivity is the target of the study. The variation between models derived for a given well location can therefore be used as a measure of uncertainty on the values obtained in each stratigraphic unit, which can be seen to increase with depth.

CSEM based Anisotropy trends in the Barents Sea.

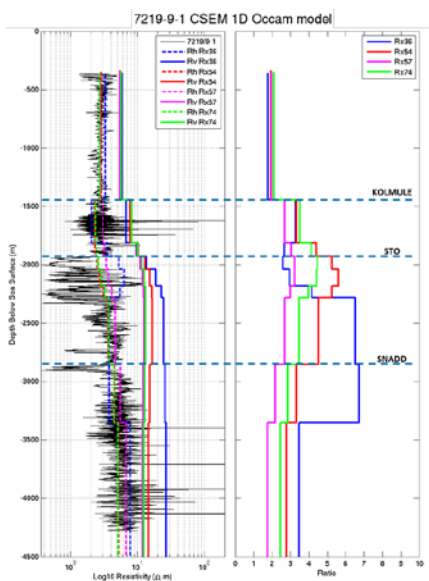


Figure 4: Comparison between 1D anisotropic inversion results around well 7219/9-1. The left plot shows the inversion results for the northern arm of receivers 01Rx036a (blue), 01Rx054a (red), 01Rx057a (magenta) and 01Rx074a (green). The dashed lines are horizontal resistivities and the solid lines are vertical resistivities. The plot on the right shows the corresponding anisotropy ratios. The insitu horizontal resistivity from well 7219/9-1 is plotted in black.

The hydrocarbon charged Skrugard well was logged using a 3-component well log and provides direct measurement of both horizontal and vertical resistivities, which allows CSEM 1D inversion results to be tied to the well and anisotropy ratios compared. The inverted horizontal resistivity shows an overall good agreement with the measured horizontal resistivity from the 3-component tool (Figure 5) in the background structure. Within the pay zone the anisotropy is significantly over-estimated. CSEM has good sensitivity to thin resistive layers in the vertical component but little sensitivity to the horizontal resistivity within such layers (Brown et al 2012). The direct implication of this characteristic is an over-estimation of electrical anisotropy in the inversion result for hydrocarbon charged units, as observed in the 1D results.

For the overburden Torsk and Kolmule formations, CSEM derived anisotropy ratios are consistent with values seen near the dry wells. However, overall the anisotropy from the 3-component well log measurement is consistently lower than the predicted anisotropy from CSEM. This is due to the different scale at which the measurements are made. In addition to intrinsic anisotropy measured at well log scale, the CSEM measurement will be sensitive to bulk anisotropy caused by layering in the sediments. This may account for some of the mismatch.

The 1D Occam inversion algorithm provides the smoothest inversion model that can fit the data. In other words, if two models fit the data equally well, the inversion algorithm will favour the model that has less structure in it. In areas where big contrasts in resistivity are expected such as near hydrocarbon discoveries for example, the smoothness constraint will result in high resistivity being spread across a wide depth interval reducing the accuracy of background resistivity, the focus of this study. Allowing a sharp change in resistivity at the top of the hydrocarbon charged layer can result in a more accurate overburden resistivity. This is also illustrated in Figure 5. Including the break in regularization at top reservoir results in a small decrease in the resistivity of the layer directly above the reservoir, which is no longer biased to higher values by the presence of the hydrocarbon. Other layers are almost unchanged. Based on this and studies at other wells, in the presence of hydrocarbon accumulations the constrained inversion results are likely to be more accurate, however the difference is small, giving confidence in the CSEM derived resistivity and anisotropy ratios in overburden layers.

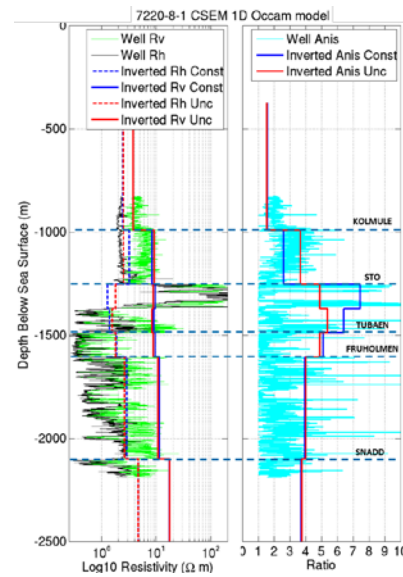


Figure 5: Well tie near the Skrugard well, showing the effect of applying a regularization break at the top Stø formation on the electrical anisotropy. Left plot shows the inversion models for the north arm of receiver 01Rx125a (the black curve is the in situ well log, the green curve is the measured vertical resistivity from the tri-axial tool), the dashed red and dashed blue models are the inverted horizontal resistivities from 1D stratigraphically constrained inversion and inversion with a break in regularization respectively, the solid red and blue models are the equivalent vertical resistivities. Right plot is the corresponding anisotropy ratios: red model from 1D stratigraphically constrained inversion, blue model from inversion with a break at top Stø, and cyan curve is the anisotropy ratio calculated from the log data.

CSEM based Anisotropy trends in the Barents Sea.

Electrical Anisotropy Maps of the Barents Sea

1D CSEM anisotropic inversion was performed for a subset of receivers near each available well location across the Barents Sea. The calculated anisotropy ratios from the inversion work were summarised on regional scale maps for Kolmule, Kolje, Knurr, Hekkingen and Snadd formations. Only those inversion results where an RMS misfit below 0.75 was achieved are included, thus limiting the uncertainty related to data fit and avoiding the inclusion of outliers in the final maps. As an example, Figure 6 shows the horizontal resistivity, vertical resistivity, anisotropy ratios and distribution of anisotropy ratios for the Kolmule formation.

There is a small degree of variability in the Kolmule formation because it is very well constrained by the CSEM data compared to the deeper/older formations. Anisotropy ratios vary from 1 to 8, with most values between 1 and 4.

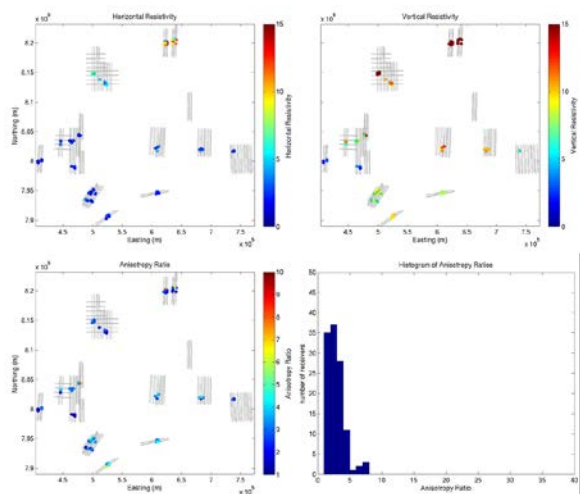


Figure 6: Maps of variation in electrical properties derived from the 1D inversion work, across all studied areas for the Kolmule formation. Upper left plot is horizontal resistivity, upper right plot is vertical resistivity, bottom left plot is anisotropy ratio and bottom right plot shows the distribution of anisotropy ratios. Each dot on the maps represents an inversion result for one arm of a CSEM receiver.

Figure 7 shows the median and standard deviation for horizontal resistivity, vertical resistivity and anisotropy ratio for areas 1 (A), 2 (B), 3 (C) and 4, 5, 6 (D) for three different formations: Torsk, Kolmule and Kolje. In general, there is an increase in anisotropy ratios with formation age. As a rule of thumb, the deeper the formation the bigger the uncertainty associated with the inverted resistivity for that formation, and therefore, the larger the uncertainty in the derived anisotropy.

High background resistivities are observed in the northern part of the Barents (Area C), for both horizontal and vertical resistivities. Because of this coupled increase, the anisotropy ratios are not affected in those areas and stay within the range of calculated ratios across the Barents Sea.

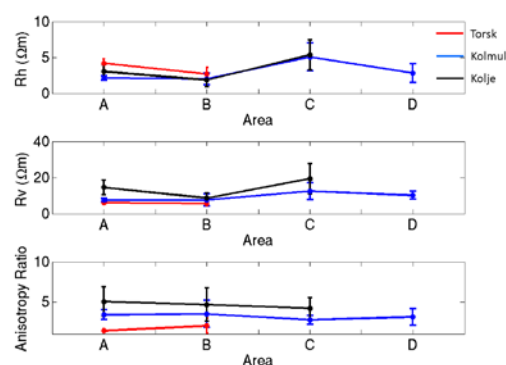


Figure 7: Median and standard deviation for horizontal resistivity (upper plot), vertical resistivity (middle plot) and anisotropy ratio (bottom plot) for areas A, B, C & D for three different formations: Torsk (red), Kolmule (blue) and Kolje (black).

Conclusion

The study presented here provides the first systematic regional study of electrical properties in the Barents Sea. Bulk overburden resistivity and anisotropy values were derived using 1D stratigraphically constrained inversion of CSEM data. By applying a stratigraphically conformant approach, we were able to efficiently determine the bulk anisotropy in each major unit. There is generally good agreement between the inverted horizontal resistivity and the logged horizontal resistivity for most wells. The inverted vertical resistivity models also show an acceptable fit to the vertical resistivity from the well where tri-axial data is available, with the difference most likely the result of the different scales (log and CSEM) at which the measurements were made. Results of 1D anisotropic modelling confirm the presence of high electrical anisotropy ratios consistent with previous observations in the Barents Sea area (Fanavoll *et al.*, 2012), and show clear trends both geographically and with formation age.

Acknowledgments

We are grateful to the ERA Consortium members (ConocoPhillips, emgs, GDF SUEZ, OMV, Repsol, Rocksource, RWE, Shell, Statoil, RWE) for support of this project. We also thank EMGS for supplying the CSEM data used in this study.

We would also like to thank Dotun Awosemo for his valuable input to this work.

EDITED REFERENCES

Note: This reference list is a copyedited version of the reference list submitted by the author. Reference lists for the 2015 SEG Technical Program Expanded Abstracts have been copyedited so that references provided with the online metadata for each paper will achieve a high degree of linking to cited sources that appear on the Web.

REFERENCES

- Constable, S. C., R. L. Parker, and C. G. Constable, 1987, Occam's inversion: A practical algorithm for generating smooth models from electromagnetic sounding data: *Geophysics*, **52**, 289–300. <http://dx.doi.org/10.1190/1.1442303>.
- Brown, V., M. Hoversten, K. Key, and J. Chen, 2012, Resolution of reservoir scale electrical anisotropy from marine CSEM data: *Geophysics*, **77**, no. 2, E147–E158. <http://dx.doi.org/10.1190/geo2011-0159.1>.
- Fanavoll, S., S. Ellingsrud, P. T. Gabrielsen, R. Tharimela, and D. Ridyard, 2012, Exploration with the use of EM data in the Barents Sea: The potential and the challenges: *First Break*, **30** Special topic.
- MacGregor, L., and J. Tomlinson, 2014, Marine controlled-source electromagnetic methods in the hydrocarbon industry: A tutorial on method and practice: *Interpretation*, **2**, no. 3, SH13–SH32. <http://dx.doi.org/10.1190/INT-2013-0163.1>.
- Ramananjaona, C., L. MacGregor, and D. Andréis, 2011, Inversion of marine electromagnetic data in a uniaxial anisotropic stratified earth: *Geophysical Prospecting*, **59**, no. 2, 341–360. <http://dx.doi.org/10.1111/j.1365-2478.2010.00919.x>.